



Research Article

**INVESTIGATION OF THE DEFORMATIONS IN A CONCRETE FACED
ROCKFILL DAM DURING STRONG GROUND MOTION**

Murat Emre KARTAL*

Izmir Demokrasi University, Engineering Faculty, İZMİR; ORCID:0000-0003-3896-3438

Received: 21.11.2017 Accepted: 04.03.2018

ABSTRACT

The aim of this paper is to delve into non-linear deformation behavior of a concrete faced rockfill (CFR) dam under strong ground motions. For this purpose, a typical CFR dam with its reservoir water is considered in the analysis. Reservoir water is modeled using the fluid finite elements based on the Lagrangian approach. Free-field surface ground motions recorded during an earthquake are deconvolved at the base of the foundation in order to simulate correctly the design motion in the earthquake analysis. The Drucker-Prager model and the multi-linear kinematic hardening model are used for concrete slab and rockfill, respectively, for materially non-linearity. Non-linear behavior of the rockfill is obtained by the uniaxial stress-strain relation. Various joints in the CFR dam are modeled considering welded and friction contact. One-dimensional surface-to-surface contact-target element pair based on the Coulomb's friction law is also used to provide the friction. The analysis expansively presents the horizontal and vertical displacements in concrete slab-rockfill interface and also horizontal displacements in dam-foundation interface. The results show that the maximum displacements appear when the friction is considered in the joints. Additionally, hydrodynamic pressure has increased the horizontal displacements of the dam. The horizontal displacements have also been increased by the effect of the non-linear behavior of the rockfill and concrete slab.

Keywords: Concrete faced rockfill (CFR) dam, Drucker-Prager model, friction contact, lagrangian approach, non-linear behavior.

1. INTRODUCTION

Numerical modeling of concrete faced rockfill (CFR) dams is very important in seismic analysis because they include dam-foundation-reservoir interaction. Besides, CFR dams also include concrete slab-rockfill, concrete slab-plinth and plinth-foundation interactions. These dams are exposed to hydrodynamic pressure on their face slab. Seismic performance of a CFR dam depends on the performance of concrete slab during earthquakes [1-6]. The concrete slab-rockfill interface, which is one of the most important factor affecting the dam behavior, is usually determined considering friction or welded contact [5-11]. Besides, in the recent years, some researches indicate that hydrodynamic pressure on the concrete face slab may induce serious issues that are also investigated in terms of the response of rockfill in a CFR dam [6,8-9,12-13].

This study comprehensively investigates non-linear displacement behavior of a CFR dam under to deconvolved strong ground motions. Numerical solutions within the scope of the paper

* Corresponding Author: e-mail: murat.kartal@idu.edu.tr, tel: (232) 260 10 01 / 417

are based on the finite element analysis. Viscous dampers are used at foundation and reservoir water boundaries to represent non-reflecting boundary conditions. Finite element model includes dam-foundation-reservoir interaction. Reservoir water effects on the face slab are modeled using the two-dimensional (2D) fluid finite elements based on the Lagrangian approach. Welded and friction contact are used in the interaction surfaces of the CFR dam. One-dimensional contact-target element pairs based on the Coulomb's friction law are considered to describe friction in the joints. Materially non-linear analyses consider the Drucker-Prager model for concrete slab and the multi-linear kinematic hardening model for rockfill. The uniaxial stress-strain relationship of the rockfill is obtained from the shear modulus-shear strain relationship of the gravels composed by Rollins et al. [14]. All numerical analyses also include geometrically non-linearity.

2. CONTACT MECHANICS

Structural response is mostly depended on contact between discrete systems. Contact problems may include small and large deformations. Consider X^1 and X^2 nodes on B^a bodies in Fig. 1 which have different initial conditions. After deformations, $\varphi(X^2) = \varphi(X^1)$, these nodes come into same position in the Γ_c boundaries (Fig. 1). Consider B^a elastic bodies, $a=1,2$, Γ^a boundary of the B^a body consists of: Γ_σ^a with prescribed surface loads, Γ_u^a with prescribed displacements and Γ_c^a in which B^1 and B^2 bodies come into contact [15].

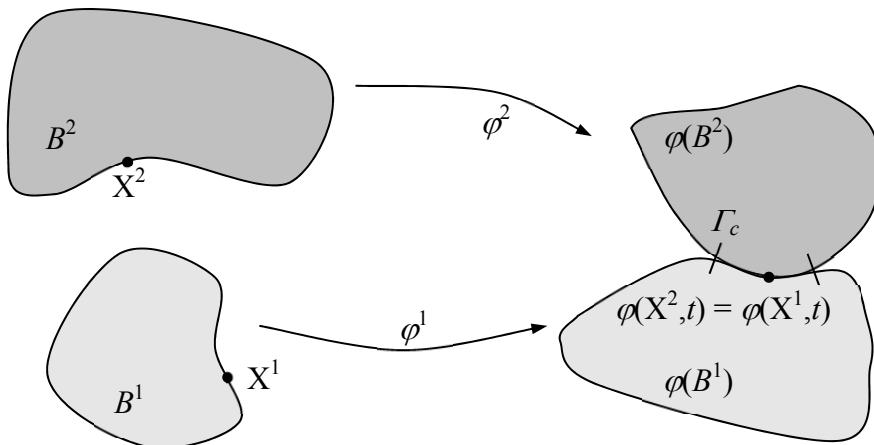


Figure 1. Finite deformation contact [15]

2.1. Constraint Formulation

The mathematical condition for non-penetration is stated as $g_N \geq 0$ which precludes the penetration of body B^1 into body B^2 . Here, g_N is named as normal gap. When g_N is equal to zero, contact occurs. In this case, the associated normal component p_N^1 of the stress vector,

$$\mathbf{t}^1 = \boldsymbol{\sigma}^1 \bar{\mathbf{n}}^1 = p_N^1 \bar{\mathbf{n}}^1 + t_T^{1\beta} \mathbf{a}_\beta^{-1} \tag{1}$$

must be non-zero in the contact interface. In the upper equation $t_T^{1\beta}$ tangential stress is zero in the case of frictionless contact. If the bodies come into contact, $\mathbf{g}_N = \mathbf{0}$ and $p_N < 0$ where p_N is normal contact pressure. If there is a gap between the bodies, $\mathbf{g}_N > \mathbf{0}$ and $p_N = 0$. This leads to some statements which are known as Hertz-Signorini-Moreau conditions [15].

$$\mathbf{g}_N \geq \mathbf{0}; \quad p_N \leq \mathbf{0}; \quad p_N \mathbf{g}_N = \mathbf{0} \tag{2}$$

In Eq. (1) Cauchy theorem is given by Cauchy stress. Correspondingly, the stress vector can be written two different ways for nominal stresses or \mathbf{P} first Piola-Kirchhoff stress.

$$\mathbf{t} = \boldsymbol{\sigma} \mathbf{n} \quad \text{or} \quad \mathbf{T} = \mathbf{P} \mathbf{N} \tag{3}$$

2.2. Treatment of Contact Constraints

There are various methods that can be applied to incorporate the contact constraints into the variational formulation. When the contact interface is known, the weak form can be written as equality.

$$\sum_{\gamma=1}^2 \left\{ \int_{B^\gamma} \boldsymbol{\tau}^\gamma \cdot \text{grad } \eta^\gamma dV - \int_{B^\gamma} \bar{\mathbf{f}}^\gamma \cdot \eta^\gamma dV - \int_{\Gamma_\sigma^\gamma} \bar{\mathbf{t}}^\gamma \cdot \eta^\gamma dA \right\} + C_c = 0 \tag{4}$$

Here, C_c is the contact contributions related to the active constraint set. $\eta^\gamma \in V$ is named as test function or virtual displacement and which is zero at the boundary Γ_ϕ^γ where the deformations are prescribed. $\boldsymbol{\tau}^\gamma$, $\bar{\mathbf{f}}^\gamma$ and $\bar{\mathbf{t}}^\gamma$ are the Kirchhoff stress, the body force of body B^γ and the surface traction applied on the boundary of B^γ , respectively.

There are several different variants for the formulation of C_c . One of the methods which regularize the non-differentiable normal contact and friction terms, is Augmented Lagrangian Method, used in this study. The main idea of this method is to combine either the penalty method or the constitutive interface laws with Lagrange multiplier methods. This method was applied to contact problems for frictionless contact [16,17] and then this approach was extended to large displacement contact problems including friction [18-19].

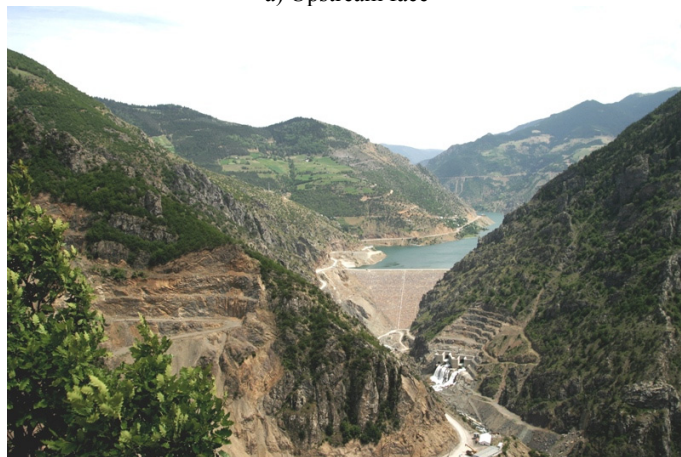
3. NUMERICAL MODEL OF A CFR DAM

3.1. Torul Dam

The Torul CFR Dam is located on the Harsit River, approximately 14 km northwest of Torul, in Gumushane Province (Fig. 2). General Directorate of State Hydraulic Works (DSI) completed the construction of this dam in 2007 [20]. The main aim of this project was power generation. The volume of the dam body is $4.6 \times 10^6 \text{ m}^3$ and the surface area of the reservoir at the normal water level is 3.62 km^2 . The annual total power generation capacity is 322.28 GW. The length of the dam crest is 320 m, the width of the dam crest is 12 m, and the maximum height and base width of the dam crest are 142 m and 420 m, respectively. The maximum water level is 137.5 m. The thickness of the concrete slab is 0.3 m at the crest level where 0.7 m at the foundation level. The largest cross section and the dimensions of the dam are shown in Fig. 3.



a) Upstream face



b) Downstream face

Figure 2. The view of Torul CFR Dam [20].

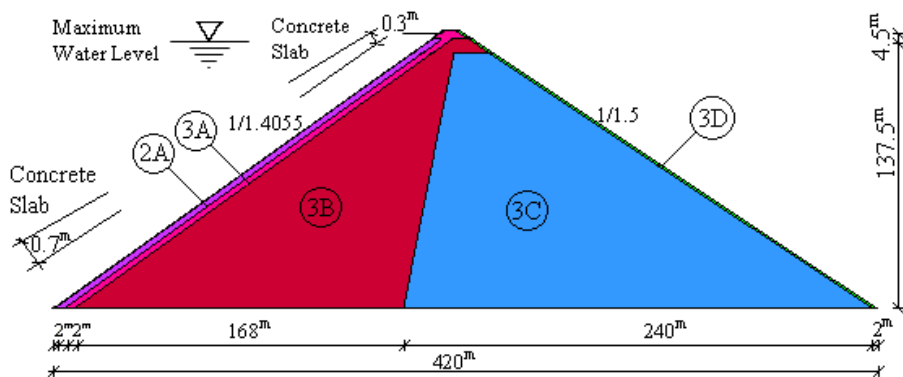


Figure 3. The largest cross section and the dimensions of the Torul CFR dam [20].

3.2. Material Properties of Torul Dam

The Torul dam which figures a typical CFR dam body, consists of a concrete face slab, transition zones (2A, 3A), rockfill zones (3B, 3C) and riprap (3D), respectively, from upstream to downstream. These zones are arranged from thin granules to thick particles in the upstream-downstream direction. The geologic investigations show Spilite (below), limestone (middle) and volcanic tufa (upper) existence in the foundation soil [20]. The material properties of the dam and foundation soil used in linear and non-linear analysis are given in Table 1. This study considers the Young's modulus of 3C zone as 200 MPa [7] because the rockfill is well graded, well compacted and constituted of materials with high compression modulus. The material properties of rockfill zones are chosen considering that the elastic constant increases with maximum particle size for alluvial material whereas it decreases with maximum particle size for quarried material [21]. The cohesion and the angle of internal friction of the concrete are assumed to be 2.50 MPa and 30°, respectively. In addition, the concrete has a tensile strength of 1.6 MPa and a compression strength of 20 MPa [22]. The bulk modulus and mass density of the reservoir water are 2.07×10^3 MPa and 1000 kg/m³, respectively.

Table 1. Material properties of Torul CFR dam

Material	*D _{max} (mm)	Material Properties		
		Young's Modulus (10 ⁷ kN/m ²)	Poisson's Ratio	Mass Density (kg/m ³)
Concrete	-	2.800	0.20	2395.5
2A (sifted rock or alluvium)	150	0.040	0.36	1880.0
3A (selected rock)	300	0.030	0.36	1870.0
3B (quarry rock)	600	0.025	0.32	1850.0
3C (quarry rock)	800	0.020	0.32	1850.0
3D (selected rock)	1000	0.018	0.26	1800.0
Foundation Soil (volcanic tufa)	-	1.036	0.17	2732.9
Foundation Soil (limestone)	-	1.206	0.18	2834.8
Foundation Soil (Spilite)	-	1.387	0.18	2834.8

*Maximum particle size

3.3. Finite Element Model of Torul Dam

The 2D finite element model of the dam is shown in Fig. 4. The model includes dam-foundation-reservoir interaction. This model also includes plinth. The solid elements used in the finite element model have four nodes and 2×2 integration points; the fluid elements have four nodes and 1×1 integration point. Element matrices are computed using the Gauss numerical integration technique. Dam-foundation-reservoir interaction model involves 47 numbers of couplings. The coupling length is set as 1 mm at the reservoir-dam and reservoir-foundation interfaces. The main purpose of the couplings is to maintain equal displacements between the opposite nodes in the normal direction to the interface. The finite element model contains various joints for the connections of different sections of the dam. If each combination of the contact-target elements defined in the opposite surfaces, is assumed as a contact pair, so totally 72 contact pairs are defined in the joints of the dam.

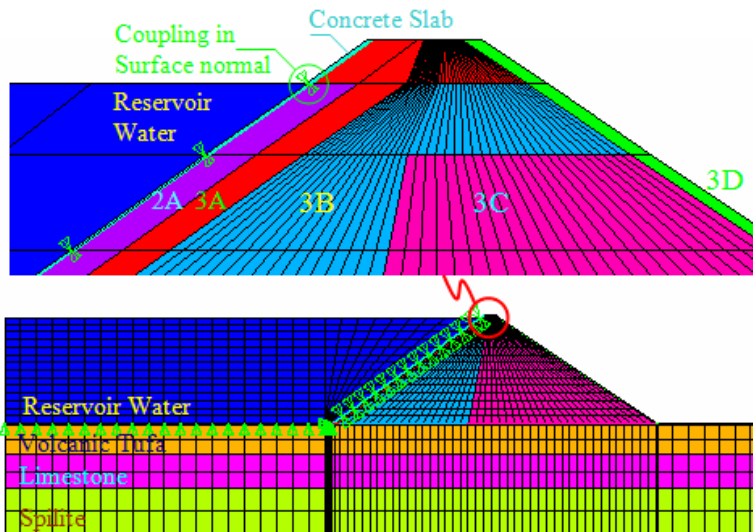


Figure 4. Two-dimensional finite element model of Torul Dam including reservoir water.

Concrete slab, transition zones, rockfill zones and riprap are included in the finite element model of the dam body. Because the soil layers lay one inside the other, there is not a recognizable point for geometric separation. However, a three-layered foundation model is designed considering experimental results obtained from soil samples.

In the finite element modelling the dam is assumed as the crest is 12 m wide, the maximum height of the dam and maximum water level are 142 m and 137.5 m, respectively. The length for both the reservoir water and foundation soil in the upstream direction is considered as three times of the dam height which is in good agreement with Bayraktar et al. (2010). In addition, the total height of the soil layers and soil length in the downstream direction are taken into account as the dam height.

3.4. Structural Connections in a CFR Dam

There are various joints in a CFR dam. The connections in these joints are generally modeled considering welded and friction contact. Welded contact defines common nodes in the contact interface. Therefore, stress or displacement transmission is not possible in this interface, since the same displacement and common stress components in the related node of adjacent elements are obtained (Fig. 5). However, interface or contact elements are required for friction contact (Fig. 5). Interface elements, which are four or six noded finite elements for plane systems, provide friction behavior by defined transverse shear stiffness. In the other case, two or three noded contact element pairs define friction. In this study, two noded surface-to-surface contact and target elements are used. In the course of using this element, if contact occurs, sliding appears depending on the maximum shear stress allowed and friction coefficient.

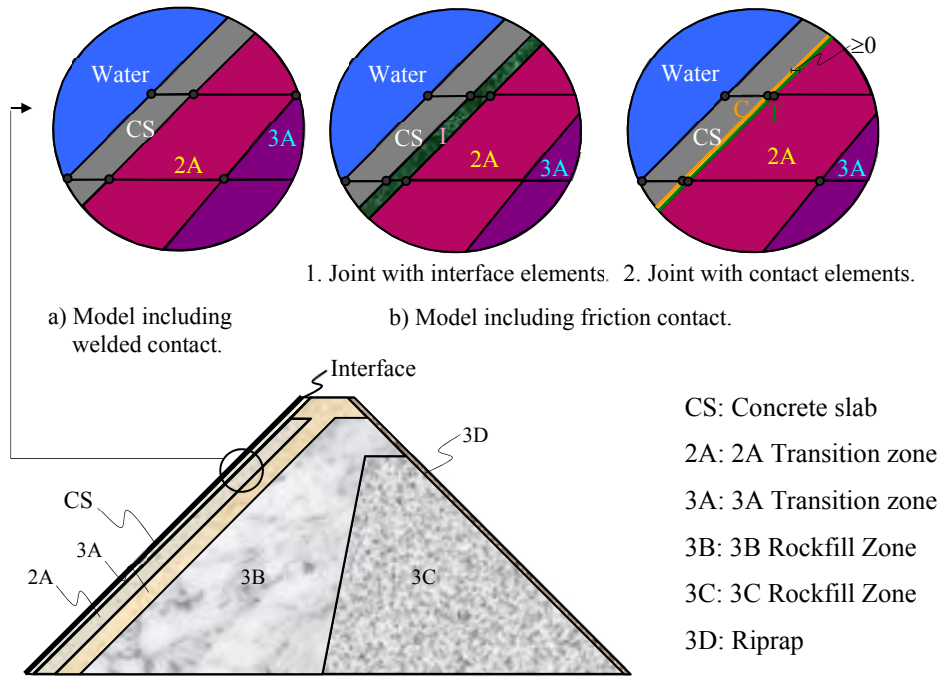


Figure 5. Schematic representation of connection types in concrete slab-rockfill interface.

If the material properties of the adjacent media are different, the connection in their interface should be formed with different nodes. It can be concluded that, for a CFR dam, concrete slab-rockfill, rockfill-foundation, concrete slab-plinth and plinth-foundation interfaces can be regarded. Therefore, friction in these interfaces can provide more realistic results. This study considers Coulomb's friction law in these interfaces.

3.5. Non-linear Behavior of CFR Dams

Permanent deformations are observed in the earthfill dams under strong ground motions. This refers that the response of the earthfill dams are actually not linear. Therefore, non-linear response of the dams should be also taken into consideration in the numerical analysis. Non-linear response of rockfill and foundation rock is determined by the multi-linear kinematic hardening model. In this method, uniaxial stress-strain curve of the non-linear material is required. This curve can be determined by shear modulus-shear strain relationship for rock and rockfill materials. Rollins et al. [14] produced the best-fit hyperbolic curve defining G/G_{max} versus cyclic shear strain relationship for gravelly soils based on testing by 15 investigators (Fig. 6). This study considers the best curve produced by Rollins et al. (1998) for rockfill. In addition, shear modulus-shear strain relation for rock soils obtained from experimental studies by Schnabel et al. [23] is used for rock foundation (Fig. 7). The uni-axial stress-strain curves for rockfill and foundation soil are determined by using these curves as shown in Figs. 8 and 9. Besides, non-linear response of the concrete slab is determined according to the Drucker-Prager material model.

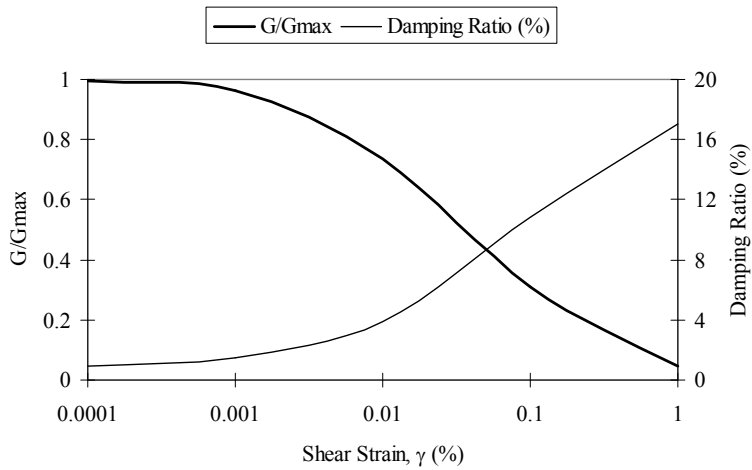


Figure 6. Normalized shear modulus-shear strain and damping ratio relationships for gravels [14].

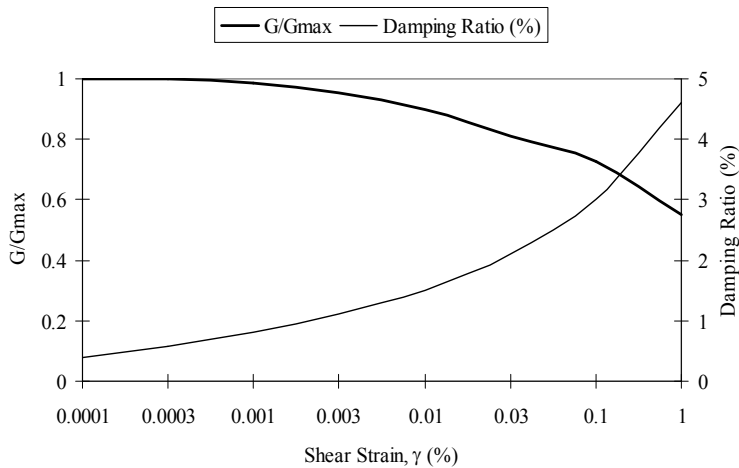


Figure 7. Normalized shear modulus-shear strain and damping ratio relationships for rocks [23].

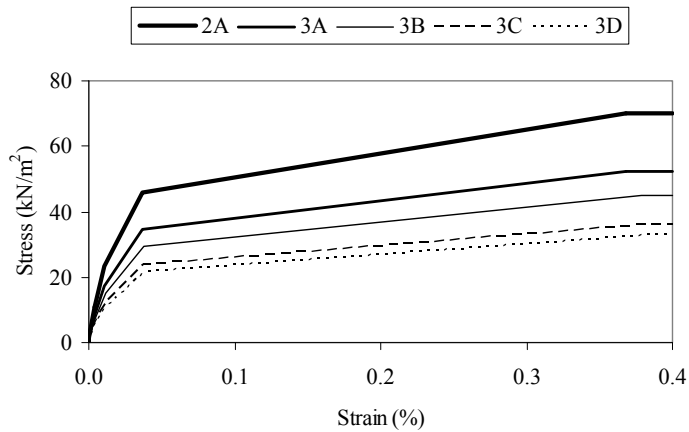


Figure 8. The uniaxial stress-strain relationship for rockfill.

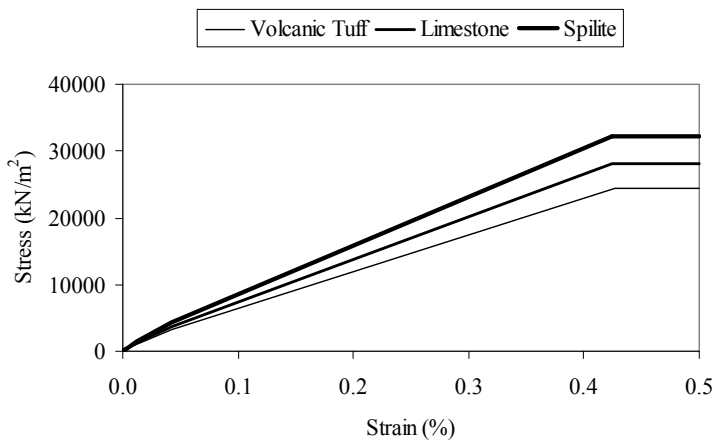


Figure 9. The uniaxial stress-strain relationship for foundation rock.

Finite element model built for friction contact considers Coulomb's friction law in the structural connections. Contact elements realize it. Those are the contact pairs defined mutually as contact element and target element. "No separation" contact model is preferred in the concrete slab-rockfill, rockfill-foundation and plinth-foundation interfaces. However, "standard" contact model is preferred in the concrete slab-plinth interface. In the standard contact model, the structural element behind the contact element may slide over and leaves from the structural element behind the target element. However, though the contact surface does not separate from the target surface, it may slide over the target surface in the no separation contact model.

3.6. Analysis Cases

Numerical solutions are performed according to three case analyses which contain geometrically and materially non-linear analyses as given in Table 2. The aim of these cases is to reveal the effect of the materially non-linear behavior of the rockfill and concrete slab on the earthquake response of the dam.

Table 2. Numerical analysis cases

Cases	Response					
	Geometrically			Materially		
	Concrete slab	Rockfill	Soil	Concrete slab	Rockfill	Soil
Case 1	Non-linear	Non-linear	Non-linear	Linear	Linear	Linear
Case 2	Non-linear	Non-linear	Non-linear	Linear	Non-linear	Non-linear
Case 3	Non-linear	Non-linear	Non-linear	Non-linear	Non-linear	Non-linear

4. DECONVOLVED GROUND MOTION MODEL

4.1. The Deconvolved-Base Rock Input Model

Free-field surface motions recorded during earthquakes reflect to the characteristics of underlying soil layers at the recording site [24,25]. Real ground response problems usually involve soil deposits with layers of different stiffness and damping characteristics with boundaries at which elastic wave energy will be reflected and/or transmitted [25]. The theory considers the responses associated with vertical propagation of shear waves through the linear viscoelastic system. A soil deposit is consisting of n horizontal homogeneous and isotropic layers where the nth layer is the bedrock is shown in Fig. 10.

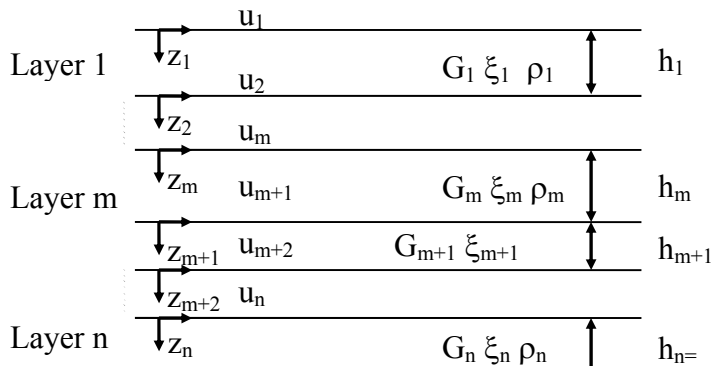


Figure 10. One-dimensional system.

Vertical propagation of shear waves through the system in Fig. 10 will cause only horizontally displacements. Introducing a local coordinate system z for each layer, the displacements at the top and bottom of layer m will be:

$$u_m(z_m, t) = \left(A_m \cdot e^{ik_m^* z_m} + B_m \cdot e^{-ik_m^* z_m} \right) e^{i\omega t} \tag{5}$$

The shear stresses at the top and bottom of layer m are:

$$\tau_m(z_m, t) = ik_m^* G_m^* \left(A_m \cdot e^{ik_m^* z_m} - B_m \cdot e^{-ik_m^* z_m} \right) e^{i\omega t} \tag{6}$$

where, values of z_m are taken into account as zero and h_m . The transfer function $F_{ij}(\omega)$ between the displacements at level i and j is defined by Eq. 7;

$$F_{ij}(\omega) = \frac{|u_i|}{|u_j|} = \frac{a_i(\omega) + b_i(\omega)}{a_j(\omega) + b_j(\omega)} \quad (7)$$

where a_i and b_i are the transfer functions for the case $a_1 = b_1 = 1$. Eq. 7 describes the amplification of accelerations and velocities. The transfer function, $F_{ij}(\omega)$, can be found between any two layers in the system. Hence, if the motion is known in any one layer in the system, the motion can be computed in any other layer [23].

4.2. Ground motion record

The reliability of the CFR dam is determined by deconvolution of the ground motion data. North-South component of the 1992 Erzincan earthquake with peak ground acceleration (PGA) of 0.515 g is used in the analysis [26]. The earthquake record is deconvolved at the base of the rock foundation in consideration of three foundation layers, by using SHAKE91 [27]. The earthquake record obtained at the ground surface and the deconvolved earthquake record are shown in Fig. 11. It is noted that the PGA of the deconvolved accelerogram is lower than the free-surface accelerogram.

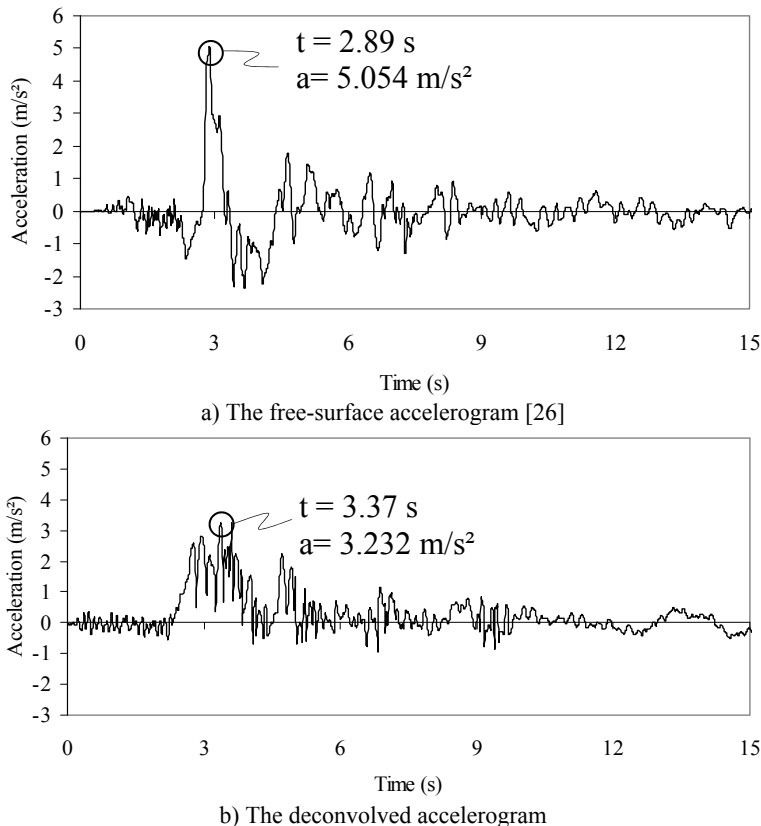


Figure 11. 1992 Erzincan earthquake record.

5. NUMERICAL RESULTS

At this part of the analysis, the change of the displacements of the concrete slab, rockfill and foundation during earthquake is computed for different slab thicknesses. All the solutions were obtained by using the Newton's algorithm with ANSYS [28]. The comparisons are carried out in concrete slab-rockfill and rockfill foundation interfaces in both empty and full reservoir conditions. All comparisons are executed considering welded and friction contact in the joints.

5.1. Displacements in the CFR dam including welded contact in the joints

The horizontal and vertical displacements in the concrete slab-rockfill interface are investigated. The horizontal displacements are shown in Figs. 12-14 for the duration of the earthquake. The comparisons are carried out for empty and full reservoir conditions in different cases.

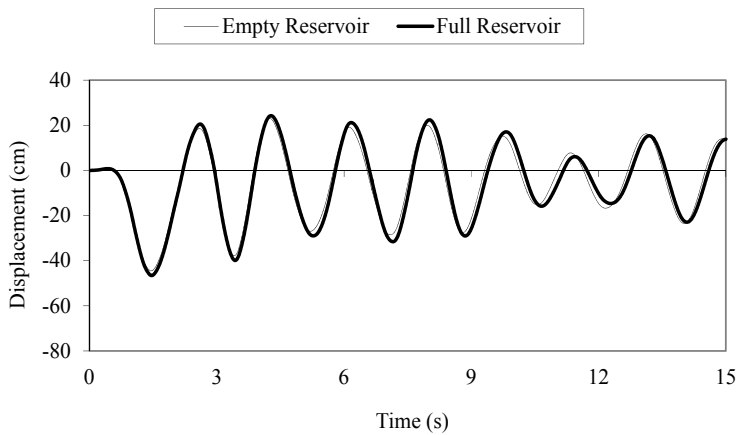


Figure 12. The horizontal displacements of the concrete slab-rockfill interface at crest for welded contact in Case 1.

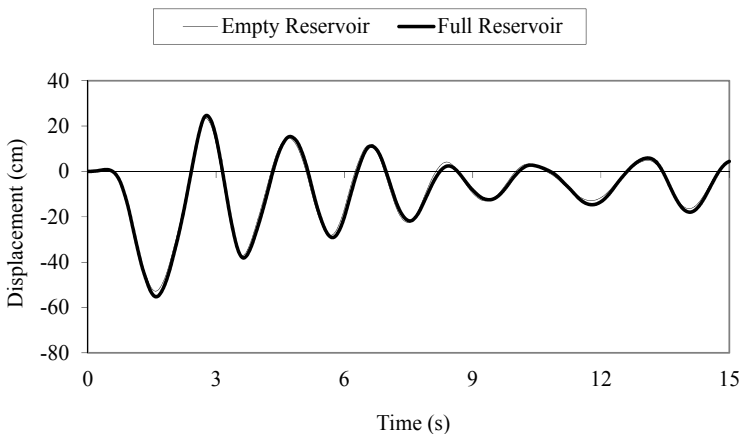


Figure 13. The horizontal displacements of the concrete slab-rockfill interface at crest for welded contact in Case 2.

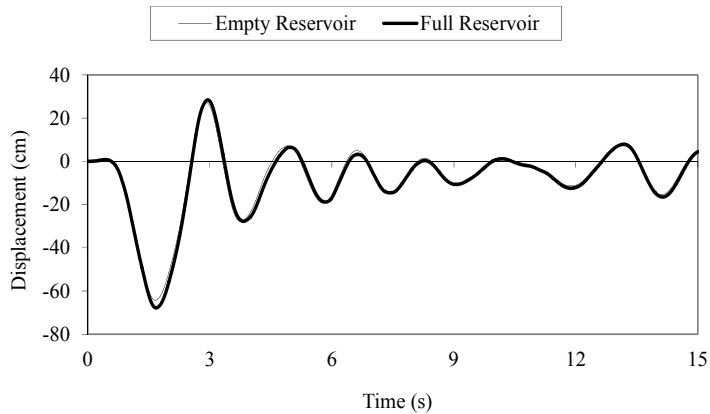


Figure 14. The horizontal displacements of the concrete slab-rockfill interface at crest for welded contact in Case 3.

The displacements in concrete slab-rockfill interface appear about the initial site during earthquake in Case 1. In this case, the horizontal displacements are higher in upstream direction than those in downstream. The displacements increase especially in upstream direction as numerical analysis considers the non-linear response of the rockfill and also foundation. In addition, the maximum horizontal displacements are obtained in Case 3 by the effect of the non-linear response of the concrete slab. The vibration axis during the seismic excitation in Cases 2 and 3 has moved toward upstream direction. Linear analyses show that effective excitations continue throughout the earthquake analysis. However, after the maximum deflections, the displacements are relatively low and leave from the initial position.

The earthquake response of the CFR dam including welded contact in the joints indicates that hydrodynamic pressure increases the displacements during the ground motion. However, linear and non-linear behaviors of the dam are in a good harmony for empty and full reservoir conditions. Numerical analyses clearly show that the maximum horizontal displacements appear in the third second of the earthquake in upstream direction.

The vertical displacements in the concrete slab-rockfill interface are also investigated and are shown for empty and full reservoir conditions in Figs. 15-17.

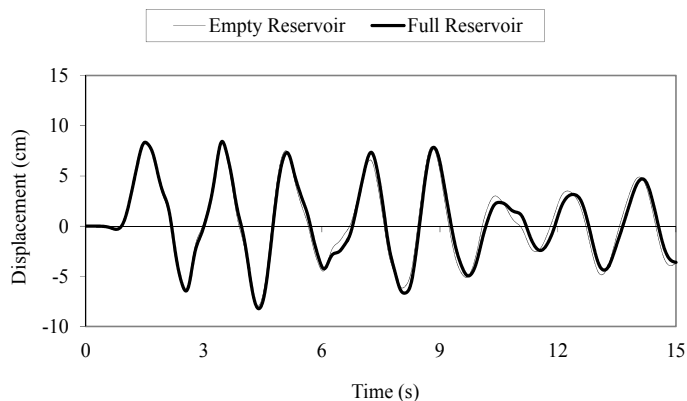


Figure 15. The vertical displacements of the concrete slab-rockfill interface at crest for welded contact in Case 1.

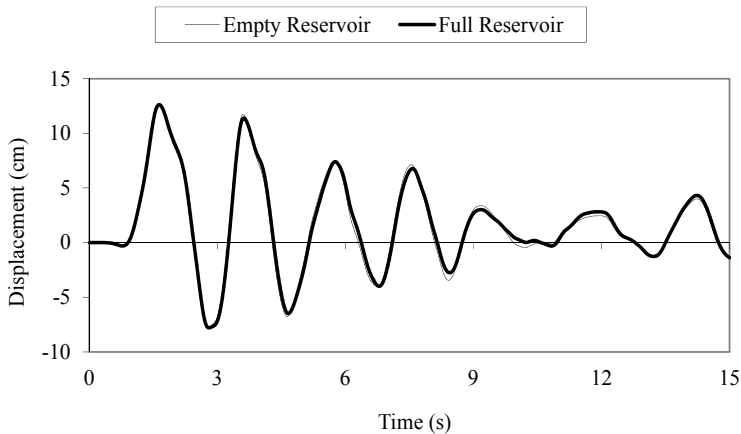


Figure 16. The vertical displacements of the concrete slab-rockfill interface at crest for welded contact in Case 2.

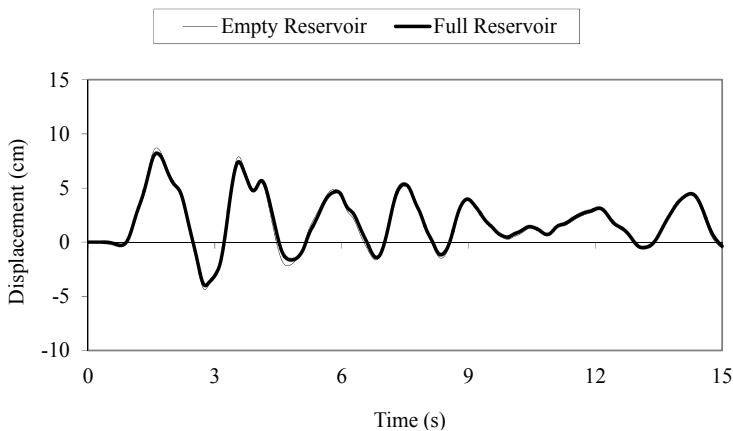


Figure 17. The vertical displacements of the concrete slab-rockfill interface at crest for welded contact in Case 3.

The hydrodynamic pressure is not effective on the vertical displacements compared to their horizontal counterparts. Besides, the vertical displacements are lower than the horizontal ones. The maximum vertical displacements also appear in the third second of the earthquake recording. The vertical displacements are increased by the non-linear response of the rockfill. However, non-linear behavior of the concrete slab has reduced them. In addition, while the vibrations occur about the initial site in Case 1, those has moved up from the initial axis in Cases 2 and 3.

5.2. Displacements in the CFR dam including friction contact in the joints

The horizontal and vertical displacements in the concrete slab-rockfill interface are shown in Figs. 18-23 and Figs. 24-29, respectively. The comparisons are made for empty and full reservoir conditions in three cases. According to given figures, concrete slab and rockfill behave as distinct from each other, owing to friction.

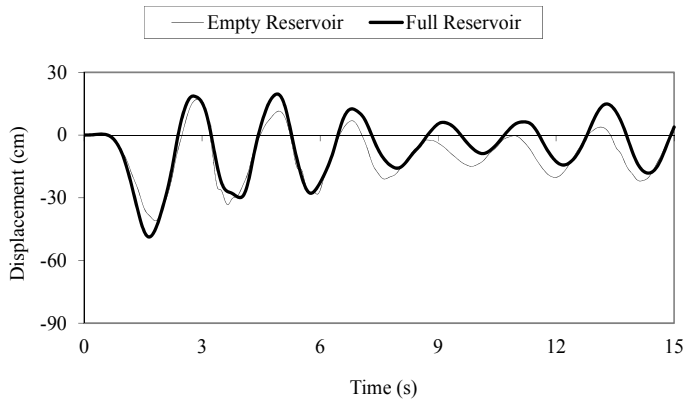


Figure 18. The horizontal displacements of the concrete slab at crest for friction contact in Case 1.

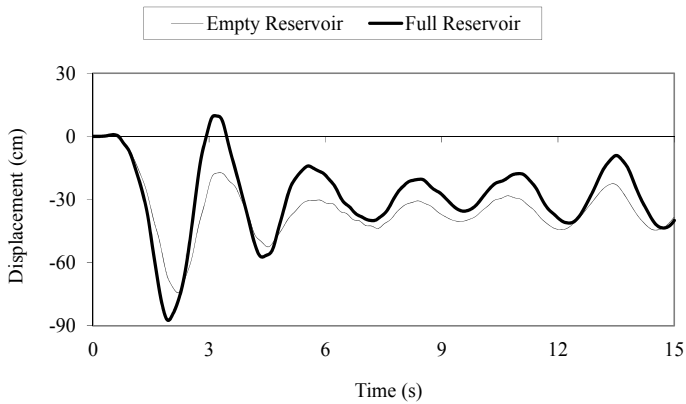


Figure 19. The horizontal displacements of the concrete slab at crest for friction contact in Case 2.

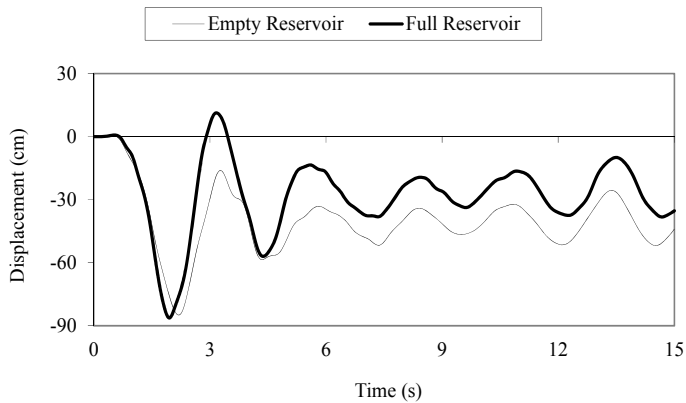


Figure 20. The horizontal displacements of the concrete slab at crest for friction contact in Case 3.

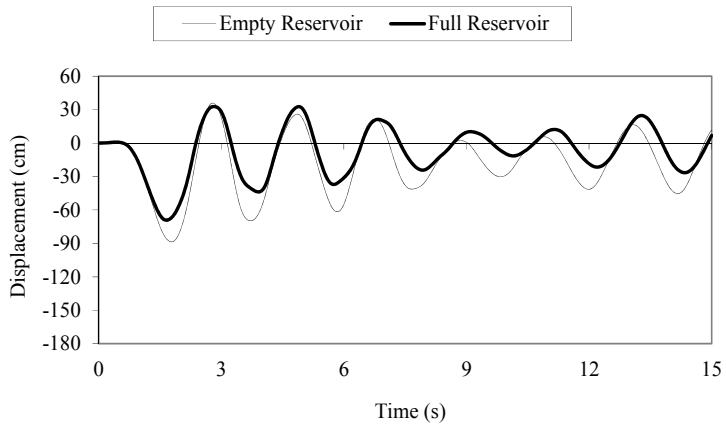


Figure 21. The horizontal displacements of the rockfill at crest for friction contact in Case 1.

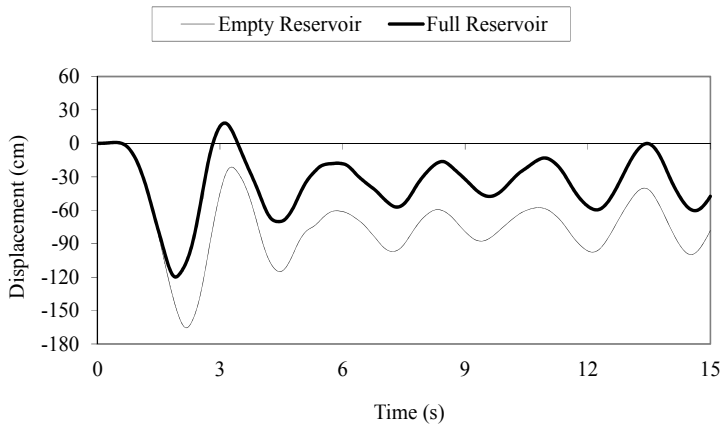


Figure 22. The horizontal displacements of the rockfill at crest for friction contact in Case 2.

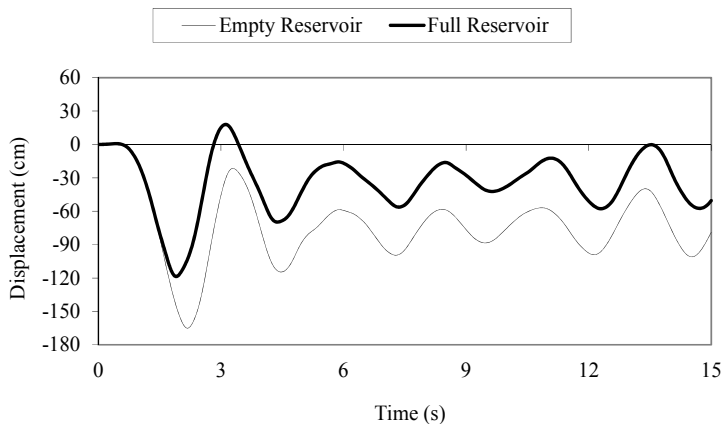


Figure 23. The horizontal displacements of the rockfill at crest for friction contact in Case 3.

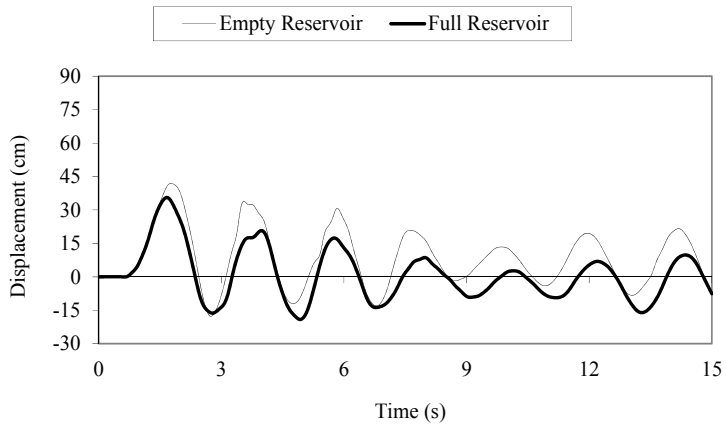


Figure 24. The vertical displacements of the concrete slab at crest for friction contact in Case 1.

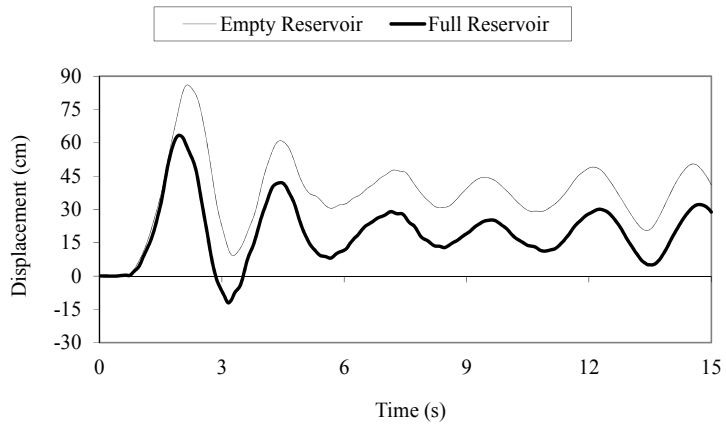


Figure 25. The vertical displacements of the concrete slab at crest for friction contact in Case 2.

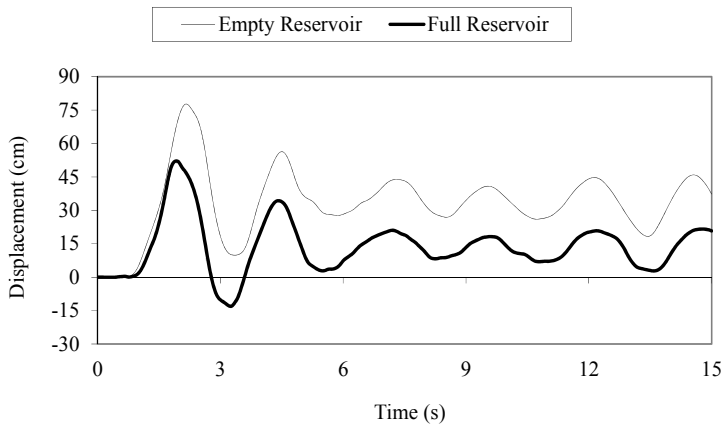


Figure 26. The vertical displacements of the concrete slab at crest for friction contact in Case 3.

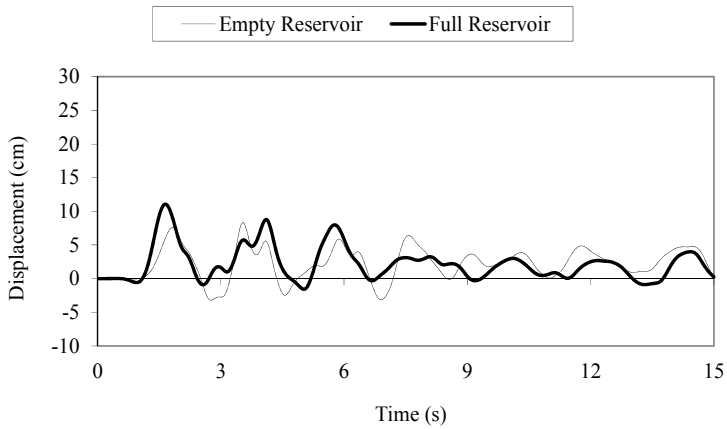


Figure 27. The vertical displacements of the rockfill at crest for friction contact in Case 1.

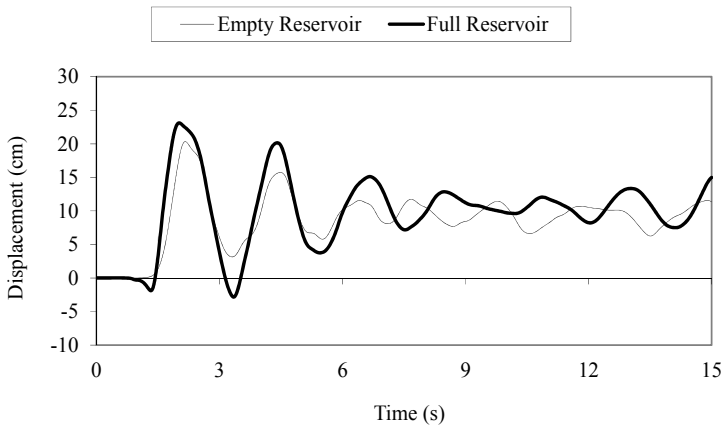


Figure 28. The vertical displacements of the rockfill at crest for friction contact in Case 2.

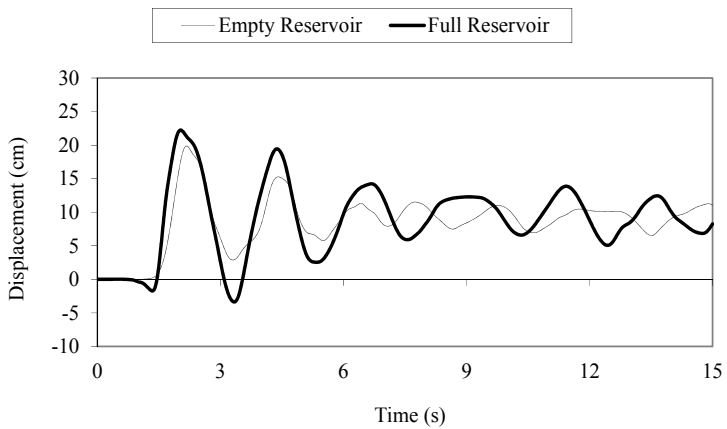


Figure 29. The vertical displacements of the rockfill at crest for friction contact in Case 3.

The change of the horizontal displacements of the concrete slab with friction contact in empty reservoir condition in Case 1, during the earthquake, resembles those for welded contact in for Cases 2 and 3. The vibration axis moved toward upstream direction and the displacements decrease with time. The horizontal displacements increase toward upstream direction in Case 2 by the effect of the non-linear response of the rockfill and foundation. In addition, the horizontal displacements of the concrete slab increase by the non-linear response of the concrete slab in empty reservoir condition in Case 3. The horizontal displacements of rockfill and concrete slab are similar to each other in Case 1. But, those are higher in full reservoir condition for the rockfill. The materially non-linearity of the rockfill further increases the horizontal displacements of the rockfill in Cases 2 and 3. The low stiffness and partially independent behavior of the rockfill from the concrete slab cause higher deformations in the rockfill.

The horizontal displacements under hydrodynamic pressure resemble the ones for empty reservoir condition in Case 1. The maximum horizontal displacements are obtained in upstream direction and those are higher in the rockfill as compared to concrete slab. Moreover, concrete slab and rockfill move toward upstream direction and make vibrations far from the initial position. Besides, no maximum horizontal displacements have appeared in Cases 2 and 3 in downstream face for concrete slab and rockfill. Only hydrodynamic pressure causes displacements in downstream direction according to initial axis in these cases during the earthquake excitement. Nevertheless, they do not represent maximum values.

The friction in the joints of the CFR dam has an obvious effect on the vertical displacements of the concrete slab-rockfill interface at crest. The concrete slab and rockfill lead to vibrations above the initial position during the earthquake because of the non-linear response of the rockfill. Concrete slab has moved downward because of the non-linear behavior of the concrete slab, but this merely affects the vertical displacements of the rockfill. Contrary to the horizontal displacements, the vertical displacements of the concrete slab are higher than those of the rockfill. While the vertical displacements of the concrete slab are below the initial position in empty reservoir condition, those of the rockfill are above the initial position in full reservoir condition. The vertical displacements increase by the non-linear response of the rockfill. The highest vertical displacements appear in third second of the earthquake.

The horizontal displacements of the rockfill and foundation during earthquake in dam-foundation interface are shown in Figs. 30-35. Consider the horizontal displacements in the bottom of the dam in empty reservoir condition; the rockfill makes higher transmitting than that of the foundation. In addition, the horizontal displacements in Cases 2 and 3 are higher than those in Case 1. The maximum displacements in the bottom of the dam occur inside the third second and then the vibrations continue with decreasing during earthquake. Such that after the horizontal displacements reach maximum value, no horizontal displacement occurs in Case 2 and 3.

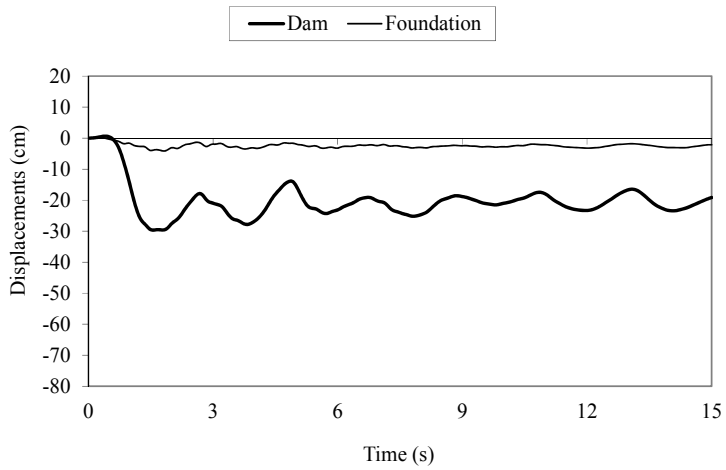


Figure 30. The horizontal displacements in dam-foundation interface for friction contact and empty reservoir condition in Case 1.

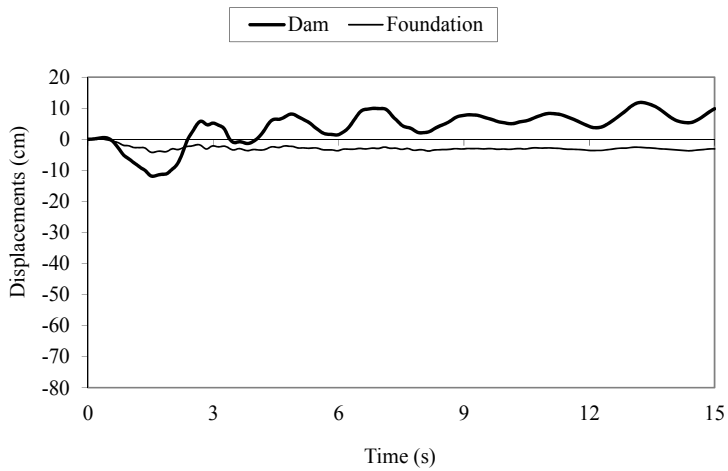


Figure 31. The horizontal displacements in dam-foundation interface for friction contact and full reservoir condition in Case 1.

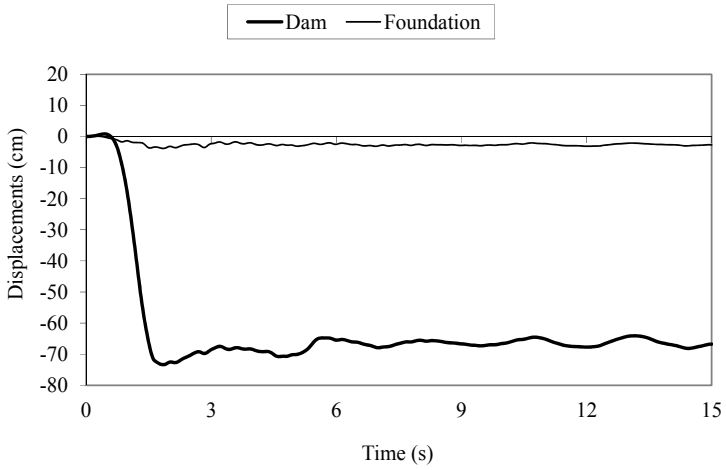


Figure 32. The horizontal displacements in dam-foundation interface for friction contact and empty reservoir condition in Case 2.

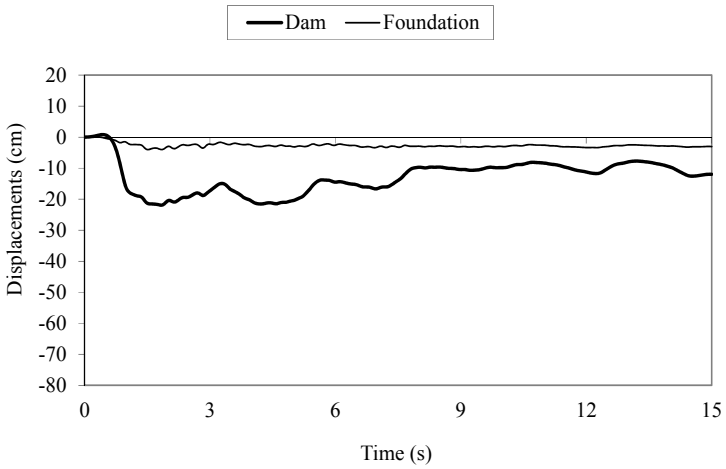


Figure 33. The horizontal displacements in dam-foundation interface for friction contact and full reservoir condition in Case 2.

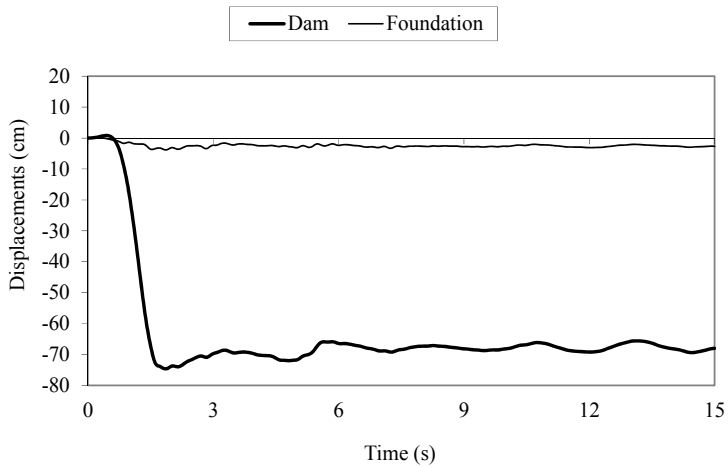


Figure 34. The horizontal displacements in dam-foundation interface for friction contact and empty reservoir condition in Case 3.

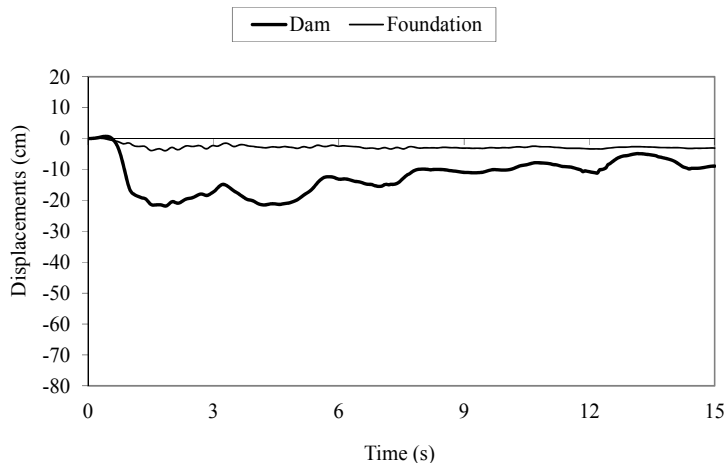


Figure 35. The horizontal displacements in dam-foundation interface for friction contact and full reservoir condition in Case 3.

The horizontal displacements at the bottom of the dam under hydrodynamic pressure are different from those in empty reservoir connection. The maximum horizontal displacements in upstream direction appear in the third second in Case 1. Then the vibration axis of the horizontal displacements moves to the downstream direction according to initial vibration axis. Cases 2 and 3 refer that non-linear response of the dam is more effective on the base translation than the effect of the rockfill and therefore base translation occur in the upstream direction according to initial position. Besides, though the reservoir water prevents the base movements, the vibrations at the bottom of the dam occur in upstream direction according to the initial position. Nevertheless, the horizontal displacements of the foundation are fairly lower than the ones of the rockfill. In addition, those are considerably less affected for the non-linear behavior of the concrete slab and rockfill.

6. CONCLUSIONS

Linear and non-linear deformation behavior of a typical CFR dam under deconvolved ground motion is studied. The Drucker-Prager model is used for concrete slab and multi-linear kinematic hardening model is utilized for rockfill in the materially non-linear analysis. The selected dam considers welded and friction contacts in the structural connections. Contact elements based on the Coulomb's friction law provide friction between the surfaces. Hydrodynamic pressure on the upstream face is considered using the fluid finite elements based on the Lagrangian approach. This study presents clearly and explains the displacements in the dam during an earthquake.

According to the analysis, non-linear response of the rockfill, thickness of concrete slab, hydrodynamic pressure and friction in the joints clearly affect the dam behavior. Hydrodynamic pressure increases the displacements of the dam. Besides, non-linear behavior of the rockfill and concrete slab also increases the displacements of the dam. The maximum horizontal and vertical displacements occurred by the effect of the friction defined in the joints of the dam. Therefore, the friction in the joints should be considered in the finite element analyses of CFR dams.

Compliance with Ethical Standards:

This study was not funded by any project with its grant number.

Conflict of Interest: The author declares that he has no conflict of interest.

REFERENCES

- [1] Seed H.B., Seed R.B., Lai S.S. and Khamenehpour, B., *Seismic Design of Concrete Face Rockfill Dams*, Proceedings of the Symposium on Concrete Face Rockfill Dams-Design, Construction and Performance, ASCE, 1985, pp. 459-478.
- [2] Priscu R., Popovici A., Stematiu D. and Stere C., *Earthquake Engineering for Large Dams*, Editura Academiei, Bucuresti and John Wiley & Sons, New York, NY, 1985.
- [3] Sherard J.L. and Cooke J.B., "Concrete-Face Rockfill Dam: I. Assessment", *Journal of Geotechnical Engineering*, ASCE, 1987; 113 (10), 1096-1112.
- [4] Gazetas G. and Dakoulas P., "Seismic Analysis and Design of Rockfill Dams – State of the Art", *Soil Dynamics and Earthquake Engineering*, 1992; 11 (1), 27-61.
- [5] Uddin N., "A Dynamic Analysis Procedure for Concrete-Faced Rockfill Dams Subjected to Strong Seismic Excitation", *Computers and Structures*, 1999; 72 (1-3), 409-421.
- [6] Bayraktar A., Kartal M.E. and Adanur S., "The Effect of Concrete Slab–Rockfill Interface Behavior on the Earthquake Performance of a CFR Dam", *International Journal of Non-Linear Mechanics*, 2011; 46 (1), 35–46.
- [7] Haeri S.M. and Karimi M. *Three-Dimensional Response of Concrete Faced Rockfill Dams to Strong Earthquakes Considering Dam-Foundation Interaction and Spatial Variable Ground Motion*, First European Conference on Earthquake Engineering and Seismology, Geneva, Switzerland, 2006, ID 1406.
- [8] Bayraktar A. and Kartal M.E., "Linear and Nonlinear Response of Concrete Slab on CFR Dam During Earthquake", *Soil Dynamics and Earthquake Engineering*, 2010; 30 (10), 990-1003.
- [9] Kartal M.E., Bayraktar A. and Başağa H.B., "Seismic Failure Probability of concrete Slab on CFR Dams with Welded and Friction Contacts by Response Surface Method", *Soil Dynamics and Earthquake Engineering*, 2010; 30(11), 1383-1399.
- [10] Kartal M.E. and Bayraktar A., "Nonlinear Earthquake Response of CFR Dam-Reservoir-Foundation Systems", *Mathematical and Computer Modelling of Dynamical Systems*, 2013; 19 (4), 353-374.

- [11] Kartal M.E. and Bayraktar A. “Non-Linear Response of the Rockfill in a Concrete Faced Rockfill Dam under Seismic Excitation”, *Mathematical and Computer Modelling of Dynamical Systems*, 2015; 21 (1), 77-101.
- [12] Bayraktar A., Altunışık A.C., Sevim B., Kartal M.E. and Türker T., “Near-Fault Ground Motion Effects on the Nonlinear Response of Dam-Reservoir-Foundation Systems”, *Structural Engineering and Mechanics*, 2008; 28 (4), 411-442.
- [13] Bayraktar A., Altunışık A.C., Sevim B., Kartal M.E., Türker T. and Bilici Y., “Comparison of Near- and Far-Fault Ground Motion Effect on the Nonlinear Response of Dam-Reservoir-Foundation Systems”, *Nonlinear Dynamics*, 2009; 58 (4), 655-673.
- [14] Rollins K.M., Evans M.D., Diehl N.B. and Daily III W.D., “Shear Modulus and Damping Relationships for Gravels”, *Journal of Geotechnical and Geoenvironmental Engineering*, 1998; 124(5), 396-405.
- [15] Wriggers P., *Computational Contact Mechanics*, 2nd Edition, Springer Verlag, Netherlands, 2006.
- [16] Wriggers P., Simo J. and Taylor R., *Penalty and Augmented Lagrangian Formulations for Contact Problems*, In Middleton, J. and Pande, G. Editors, *Proceedings of NUMETA Conference*, Balkema, Rotterdam, 1985.
- [17] Kikuchi N. and Oden J.T., *Contact Problems in Elasticity: A Study of Variational Inequalities and Finite Element Methods*, SIAM, Philadelphia, 1988.
- [18] Alart P. and Curnier A., “A Mixed Formulation for Frictional Contact Problems Prone to Newton Like Solution Methods”, *Computer Methods in Applied Mechanics and Engineering*, 1991; 92 (3), 353-375.
- [19] Laursen T.A. and Simo J.C., “Algorithmic Symmetrization of Coulomb Frictional Problems Using Augmented Lagrangians”, *Computer Methods in Applied Mechanics and Engineering*, 1993; 108 (1-2), 133-146.
- [20] DSI, *General Directorate of State Hydraulic Works, The XXII. Regional Directorate, Trabzon*, 2016.
- [21] Varadarajan A, Sharma K.G., Abbas S.M. and Dhawan A.K., “Constitutive Model for Rockfill Materials and Determination of Material Constants”, *International Journal of Geomechanics*, ASCE, 2006; 6 (4), 226-237.
- [22] TS 500, *Requirements for Design and Construction of Reinforced Concrete Structures*, 2000.
- [23] Schnabel P.B., Lysmer J. and Seed H.B., *SHAKE: A Computer Program for Earthquake Response Analysis of Horizontally Layered Sites*, Report No.EERC-72/12, Earthquake Engineering Research Centre, University of California, Berkeley, 1972.
- [24] Seed H.B., *The Influence of Local Soil Conditions on Earthquake Damage*, *Proceedings, Soil Dynamics Specialty Session, Seventh international conference of soil mechanics and foundation engineering*, Mexico, 1969.
- [25] Kramer S.L., *Geotechnical Earthquake Engineering*, Prentice-Hall Inc., First edition, New Jersey, 1996.
- [26] PEER, *Pacific Earthquake Engineering Research Centre*, <http://peer.berkeley.edu/smcat>, 2013.
- [27] Idriss I.M. and Sun J.I., *SHAKE91: A Computer Program for Conducting Equivalent Linear Seismic Response Analyses of Horizontally Layered Soil Deposits*, Center of Geotechnical Modeling Department of Civil & Environmental Engineering, University of California Davis, California, 1992.
- [28] ANSYS, *Swanson Analysis Systems Inc*, Houston PA, USA, 2016.